Journal of Molecular Structure

Synthesis, Structure and Biological Activity of 3(5)-Trifluoromethyl-1*H*-Pyrazoles Derived from Hemicurcuminoids

Carla I. Nieto[a], M. Pilar Cabildo[a], M. Pilar Cornago[a], Dionisia Sanz[a], Rosa M. Claramunt [a,*], Ibon Alkorta[b,*], José Elguero[b], José A. García[c], Ana López[c], and Darío Acuña-Castroviejo[c,*]

[a]*Departamento de Química Orgánica y Bio-Orgánica, Facultad de Ciencias, UNED, Paseo Senda del Rey, 9, 28040 Madrid, Spain*
**E-mail address*: rclaramunt@ccia.uned.es (R.M. Claramunt)
[b]*Instituto de Química Médica, Centro de Química Orgánica "Manuel Lora-Tamayo", CSIC, Juan de la Cierva, 3, 28006 Madrid, Spain*
**E-mail address*: ibon@iqm.csic.es (I. Alkorta)
[c]*Centro de Investigación Biomédica, Parque Tecnológico de Ciencias de la Salud, Universidad de Granada, Avda. del Conocimiento s/n, 18100 Armilla, Granada, Spain*
**E-mail address*: dacuna@ugr.es (D. Acuña)

Keywords: fluorinated pyrazoles; synthesis, ^{1}H, ^{13}C, ^{19}F, ^{15}N NMR; GIAO calculations; tautomerism; NOS inhibition

ABSTRACT

Six new 3(5)-trifluoromethyl-5(3)-substituted-styryl-1*H*-pyrazoles have been synthesized and their tautomerism studied in solution and in the solid state. The determination of their structures has been based on multinuclear NMR spectroscopy together with GIAO/B3LYP/6-311++G(d,p) theoretical calculations of eight structures for each pyrazole (two tautomers and four conformations). Five out of the six compounds present inhibition percentages of the iNOS isoform higher than 50%. With regard to the nNOS inhibitory activity, only two of the studied compounds show an inhibition of about 50%. Finally, concerning the eNOS, there is a compound presenting a low percentage of inhibition (40.2%) attaining in the other cases 50%.

Introduction

The interest in curcumin [(1*E*,6*E*)-1,7-bis(4-hydroxy-3-methoxyphenyl)hepta-1,6-diene-3,5-dione] [1,2,3,4,5,6,7,8,9] has prompted many structural studies on this β-diketone tautomerism [10,11,12,13,14] as well as on the synthesis and structural studies of hemicurcuminoids, compounds resulting from the replacement of one styryl branch of curcumin (2-methoxy-4-vinylphenol) by a simpler group, for instance, a phenyl group [11,15].

The discovery that the six-membered pseudoaromatic ring of the enol of curcumin [16] [(1*E*,4*Z*,6*E*)-5-hydroxy-1,7-bis(4-hydroxy-3-methoxyphenyl)hepta-1,4,6-triene-3-one] can be replaced by the five-membered ring of the heteroaromatic 1*H*-pyrazole [17] maintaining but also modifying the biological properties of curcumin, has resulted in many works [18,19,20,21,22] including two by our group [23,24] (Fig. 1).

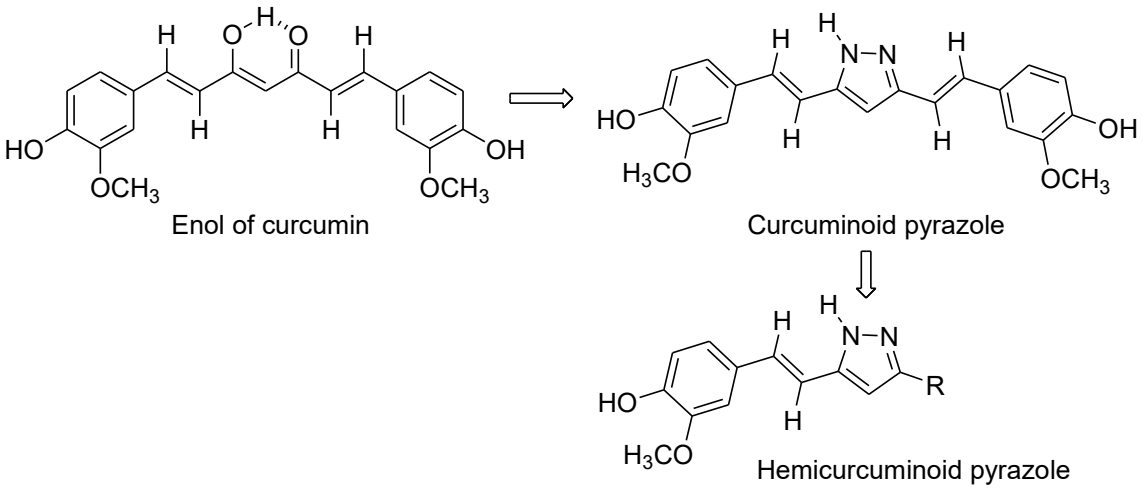

Fig. 1. The transition between curcumin and hemicurcuminoid pyrazoles [the pyrazole derived from the reaction of curcumin with hydrazine is called (mainly in pharmaceutical papers) "hydrazinocurcumine"].

Combining both approaches (hemicurcuminoids and pyrazoles) results in hemicurcuminoid pyrazoles (Fig. 1). We will now describe the case R = CF_3 (Fig. 2), that can exist in two distinct forms **a** and **b**. The atom numbering of the pyrazole ring is different in both tautomers **a** and **b**. According to the IUPAC rules [25], the numbering of the system has to be carried out in such a way that it must start at the N*H* and the two heteroatoms are given the lowest set of locants. Thus, the carbon atoms 3 and 5 exchange their numbering on going from tautomer **a** to **b**. There is ample information in the literature that a trifluoromethyl group is an interesting pharmacophore [26,27,28] even in pyrazole derivatives [29,30,31] including the well-known anti-inflammatory Celecoxib [32].

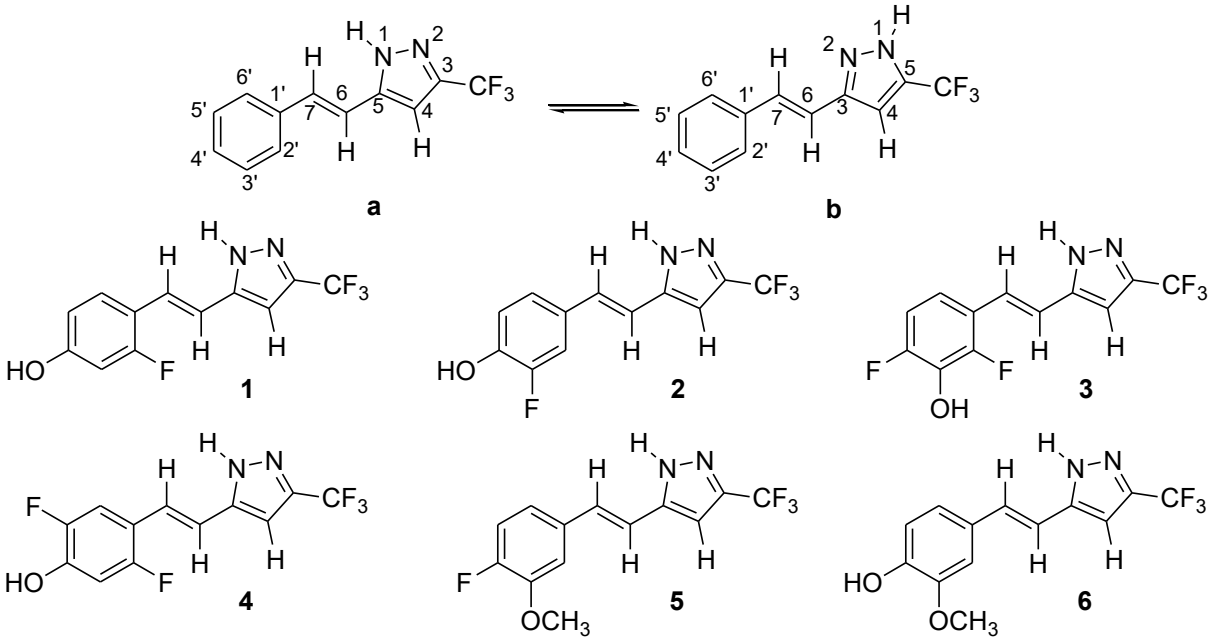

Fig. 2. The six pyrazoles studied in this work that can exist in two tautomeric forms, **a** (3-CF_3) and **b** (5-CF_3).

Experimental

General remarks

All chemicals cited in the synthetic procedures are commercial compounds. Melting points were determined by DSC with a SEIKO DSC 220 C connected to a model SSC5200H disk station. Thermograms (sample size 0.003-0.005 g) were recorded with a scan rate of 5.0 ºC/min. Column chromatography was performed on silicagel (Merck 60, 70-230 mesh) and elemental analyses using a Perkin-Elmer 240 apparatus.

Chemistry

General procedure for the preparation of pyrazole derivatives

Compounds **1**-**6** were prepared by reacting the corresponding β-diketones (1 mmol) with hydrazine hydrate 98% (1.5 mmol) in acetic acid (5 mL) [24]. After heating at reflux for 2 h the reaction mixture was poured into water. The precipitate was filtered off, washed with water and dried. In all cases pyrazoles were obtained as white solids after recrystallization from EtOH/H_2O.

*(E)-3(5)-[β-(2-fluoro-4-hydroxyphenyl)-ethenyl]-5(3)-trifluoromethyl-1H-pyrazole (**1**)*

Compound **1** was prepared from (*E*)-1,1,1-trifluoro-6-(2-fluoro-4-hydroxyphenyl)hex-5-ene-2,4-dione [11,15] (yield: 75%). Mp = 223.1 °C. Anal. Calc. for $C_{12}H_8F_4N_2O$: C, 52.95; H, 2.96; N, 10.29%. Found: C, 52.83; H, 2.96; N, 10.26%.

*(E)-3(5)-[β-(3-fluoro-4-hydroxyphenyl)-ethenyl]-5(3)-trifluoromethyl-1H-pyrazole (**2**)*

Compound **2** was prepared from (*E*)-1,1,1-trifluoro-6-(3-fluoro-4-hydroxyphenyl)hex-5-ene-2,4-dione [11,15] (yield: 88%). Mp = 204.5 °C. Anal. Calc. for $C_{12}H_8F_4N_2O$: C, 52.95; H, 2.96; N, 10.29%. Found: C, 52.98; H, 3.12; N, 10.41%.

*(E)-3(5)-[β-(2,4-difluoro-3-hydroxyphenyl)-ethenyl]-5(3)-trifluoromethyl-1H- pyrazole (**3**)*

Compound **3** was prepared from (*E*)-6-(2,4-difluoro-3-hydroxyphenyl)-1,1,1-trifluorohex-5-ene-2,4-dione [11,15] (yield: 64%). Mp = 212.6 ºC. Anal. Calc. for $C_{12}H_7F_5N_2O$: C, 49.67; H, 2.43; N, 9.65%. Found: C, 49.87; H, 2.63; N, 9.72%.

*(E)-3(5)-[β-(2,5-difluoro-4-hydroxyphenyl)-ethenyl]-5(3)-trifluoromethyl-1H-pyrazole (**4**)*

Compound **4** was prepared from (*E*)-6-(2,5-difluoro-4-hydroxyphenyl)-1,1,1-trifluorohex-5-ene-2,4-dione [11,15] (yield: 77%). Mp = 227.1 °C. Anal. Calc. for $C_{12}H_7F_5N_2O$: C, 49.67; H, 2.43; N, 9.65%. Found: C, 49.32; H, 2.50; N, 9.81%.

*(E)-3(5)-[β-(4-fluoro-3-methoxyphenyl)-ethenyl]-5(3)-trifluoromethyl-1H-pyrazole (**5**)*

Compound **5** was prepared from (*E*)-1,1,1-trifluoro-6-(4-fluoro-3-methoxyphenyl)hex-5-ene-2,4-dione [11,15] (yield: 91%). Mp = 168.0 °C. Anal. Calc. for $C_{13}H_{10}F_4N_2O$: C, 54.55; H, 3.52; N, 9.79%. Found: C, 54.32; H, 3.59; N, 9.85%.

*(E)-3(5)-[β-(4-hydroxy-3-methoxyphenyl)-ethenyl]-5(3)-trifluoromethyl-1H-pyrazole (**6**)*

Compound **6** was prepared from (*E*)-1,1,1-trifluoro-6-(4-hydroxy-3-methoxyphenyl)hex-5-ene-2,4-dione [11,15] (yield: 98%). Mp = 165.0 °C. Anal. Calc. for $C_{13}H_{11}F_3N_2O_2$: C, 54.93; H, 3.90; N, 9.86%. Found: C, 54.63; H, 3.76; N, 9.60%.

NMR measurements

Solution NMR spectra were recorded on a Bruker DRX 400 (9.4 Tesla, 400.13 MHz for ^1H, 100.62 MHz for ^{13}C, 40.54 MHz for ^{15}N and 376.50 MHz for ^{19}F) spectrometer with a 5-mm inverse-detection H-X probe equipped with a z-gradient coil (^1H, ^{13}C, ^{15}N) and with a QNP 5 mm probe (^{19}F), at 295 K. Chemical shifts (δ in ppm) are given from internal solvent, DMSO-d_6 2.49 for ^1H and 39.5 for ^{13}C, HMPA-d_{18} 2.51 to the upfield multiplet for ^1H and 35.8 for ^{13}C. External

references were used for ^{15}N and ^{19}F, nitromethane and $CFCl_3$ respectively. Coupling constants (J in Hz) are accurate to ± 0.2 Hz for ^{1}H, ± 0.6 Hz for ^{13}C and ± 0.8 Hz for ^{19}F. Typical parameters for ^{1}H NMR spectra were spectral width 6500 Hz and pulse width 7.5 µs at an attenuation level of 0 dB. Typical parameters for ^{13}C NMR spectra were spectral width 21 kHz, pulse width 10.6 µs at an attenuation level of –6 dB and relaxation delay 2 s; WALTZ-16 was used for broadband proton decoupling; the FIDs were multiplied by an exponential weighting (lb = 2 Hz) before Fourier transformation. 2D (^{1}H-^{13}C) gs-HMQC, (^{1}H-^{13}C) gs-HMBC and 2D (^{1}H-^{15}N) gs-HMQC, (^{1}H-^{15}N) gs-HMBC were acquired and processed using standard Bruker NMR software and in non-phase-sensitive mode [33]. Gradient selection was achieved through a 5% sine truncated shaped pulse gradient of 1 ms.

Solid-state ^{13}C (100.73 MHz) and ^{15}N (40.60 MHz) CPMAS NMR spectra have been obtained on a Bruker WB 400 spectrometer at 300 K using a 4 mm DVT probehead. Samples were carefully packed in a 4-mm diameter cylindrical zirconia rotor with Kel-F end-caps. Operating conditions involved 3.2 µs 90° ^{1}H pulses and decoupling field strength of 86.2 kHz by TPPM sequence. ^{13}C spectra were originally referenced to a glycine sample and then the chemical shifts were recalculated to the Me_4Si [for the carbonyl atom δ (glycine) = 176.1 ppm] and ^{15}N spectra to $^{15}NH_4Cl$ and then converted to nitromethane scale using the relationship: $\delta^{15}N$(nitromethane) = $\delta^{15}N$(ammonium chloride) – 338.1 ppm. Typical acquisition parameters for ^{13}C CPMAS were: spectral width, 40 kHz; recycle delay, 5-30 s; acquisition time, 30 ms; contact time, 2-5 ms; and spin rate, 12 kHz. In order to distinguish protonated and unprotonated carbon atoms, the NQS (Non-Quaternary Suppression) experiment by conventional cross-polarization was recorded; before the acquisition the decoupler is switched off for a very short time of 25 µs [34,35]. And for ^{15}N CPMAS were: spectral width, 40 kHz; recycle delay, 5-30 s; acquisition time, 35 ms; contact time, 2-7 ms; and spin rate, 6 kHz.

Solid-state ^{19}F (376.94 MHz) NMR spectra have been obtained on a Bruker WB 400 spectrometer using a MAS DVT BL2.5 X/F/H double resonance probehead. Samples were carefully packed in 2.5 mm diameter cylindrical zirconia rotors with Kel-F end-caps. Samples were spun at the magic angle at rates of 25 kHz and the experiments were carried out at ambient probe temperature.

The typical acquisition parameters $^{19}F\{^{1}H\}$ MAS were: spectral width, 75 kHz; recycle delay, 10 s; pulse width, 2.5 µs and proton decoupling field strength of 100 kHz by SPINAL-64 sequence; recycle delay, 10 s; acquisition time, 25 ms; 128 scans; and spin rate, 25 kHz.

The ^{19}F spectra were referenced to ammonium trifluoroacetate sample and then the chemical shifts were recalculated to the $CFCl_3$ ($\delta CF_3COO^-NH_4^+$ = –72.0 ppm).

In vitro nNOS, iNOS and eNOS activities determination

L-Arginine, L-citrulline, *N*-(2-hydroxymethyl)piperazine-*N*'-(2-ethanesulfonic acid) (HEPES), DL-dithiothreitol (DTT), leupeptin, aprotinin, pepstatin, phenylmethylsulfonyl fluoride (PMSF), hypoxantine-9-*β*-D-ribofuranosid (inosine), ethylene glycol-bis- (2 aminoethylether)-*N*,*N*,*N*′,*N*′-tetraacetic acid (EGTA), bovine serum albumin (BSA), Dowex-50W (50 X 8–200), FAD, NADPH and 5,6,7,8-tetrahydro-L-biopterin dihydrocloride (H_4-biopterin) were obtained from Sigma–Aldrich Química (Spain). L-[^{3}H]-arginine monohydrochloride (45-70 Ci/mmol, 1 mCi/mL) was obtained from Perkin Elmer Life Sciences (Spain). Tris(hydroxymethyl)aminomethane (Tris-HCl) and calcium chloride were obtained from Merck (Spain). Calmodulin from bovine brain was obtained from Alexis Biochemicals (Enzo Life Sciences, Grupo Taper, Seville, Spain), recombinant iNOS (specific activity of 3.9 µmol/min/mg protein) and eNOS (Cayman Chemical, specific activity 3 µmol/min/mg protein) were obtained from Cayman Chemical (Vitro S.A, Madrid, Spain).

For nNOS activity determination, C57BL/6 mice (3-months old, 25-30 g) (The Jackson Laboratory, Bar Harbor, Maine, USA) were housed in the animal facility of the University of Granada under specific pathogen-free conditions, and in a controlled 12-h light/dark cycle at 22 ± 2ºC. Mice had unlimited access to water and rodent chow until the day of the experiment. All

experiments were performed according to the Spanish Government Guide and the European Community Guide for animal care. The experimental paradigm was published elsewhere [36]. Briefly, mice were killed by cervical dislocation and brain was quickly collected, washed, and homogenized in an ice-cold buffer (51 mM Tris, 1 mM DTT, 10 µg/mL leupeptin, 10 µg/mL pepstatin, 10 µg/mL aprotinin, 1 mM PMSF, pH 7.6). The crude homogenate was centrifuged twice at 1000 *g* at 4 ºC, and sonicated (10 s x 6). Aliquots of the supernatant were either stored at -80ºC for total protein quantification [37] or immediately used for NOS activity measurement. For iNOS and eNOS activity determination, recombinant enzymes were used.

NOS activity was measured following the conversion of L-^{3}H-arginine to L-^{3}H-citrulline according to the Bredt *et al*. protocol [38]. Enzyme activity was referred as pmol L-^{3}H-citrulline/min/mg prot. The final incubation volume was 100 µL and consisted of 10 µL of an aliquot of homogenized brain (for nNOS measurement) or recombinant enzyme (for iNOS or eNOS measurement) added to a buffer with a final concentration of 25 mM Tris–HCl, 0.5 mM DTT, 30 µM H_4-biopterin, 10 µM FAD, 0.5 mM inosine, 1 mg/mL BSA, 0.5 mM $CaCl_2$ (or 1 mM for iNOS measurement), 10 µM L-arginine, and 50 nM L-[^{3}H]-arginine, 10 µg/mL calmodulin (only for constitutive isoforms), at pH 7.6. Final volume also included 10 µL of each pyrazole compound dissolved in DMSO to give a final concentration of 50 µM. The activity of the different NOS isoforms was also assayed in the presence of DMSO to discard any non-specific effect of the compounds, proving that the DMSO had no significant effects on the measured NOS activity. The reaction was started by the addition of 10 µL of NADPH (0.75 mM final) and continued for 30 min at 37 ºC. Control incubations were performed by the omission of NADPH. The reaction was stopped adding 400 µL of cold 0.1 M HEPES, 0.1 M EGTA, and 0.175 mg/mL L-citrulline, pH 5.5. The reaction mixture was decanted onto a 2 mL column packet with Dowex-50W ion-exchange resin (Na^+ form) and eluted with 1.2 mL of water. L-^{3}H-citrulline was quantified by liquid scintillation counting in a Beckman LS-6000 system (Beckman Coulter, Fullerton, CA, USA). The retention of L-[^{3}H]-arginine in this process was greater than 98%. Specific enzyme activity was determined by subtracting the control value. Statistical analysis: Data are expressed as the mean ± SEM. Statistical analysis was performed by Student's t-test. A $P < 0.05$ was considered statistically significant.

Computational details

The geometry of the systems has been optimized at the B3LYP [39,40,41]/6-311++G(d,p) [42,43] computational level. According to the calculations, the molecules correspond to energy minima ($\lambda = 0$ where λ is the number of negative eigenvalues of the Hessian matrix for a given stationary point) on the PES. All the calculations have been carried out with the Gaussian-09 program [44]. Theoretical calculations of absolute shieldings (σ, ppm) and their transformation into chemical shifts (δ, ppm) were carried out at the GIAO/B3LYP/6-311++G(d,p) level as described in previous papers [45,46,47,48]. The same geometries have been used for the calculation of the spin-spin indirect coupling constant at the B3LYP/6-311++G(d,p) level with the GIAO method.

Results and discussion

Synthesis

The synthetic pathway followed for the preparation of pyrazoles **1-6** is depicted in Fig. 3. First, β-diketones were obtained from 1,1,1-trifluoropentane-2,4-dione by reaction with 2-fluoro-4-hydroxybenzaldehyde, 3-fluoro-4-hydroxybenzaldehyde, 2,4-difluoro-3-hydroxybenzaldehyde, 2,5-difluoro-4-hydroxybenzaldehyde, 4-fluoro-3-methoxybenzaldehyde and 3-methoxy-4-hydroxybenzaldehyde according to a general method described elsewhere [15]. Finally condensation of the β-diketones with hydrazine hydrate in acetic acid yielded the corresponding pyrazoles in quantitative yields.

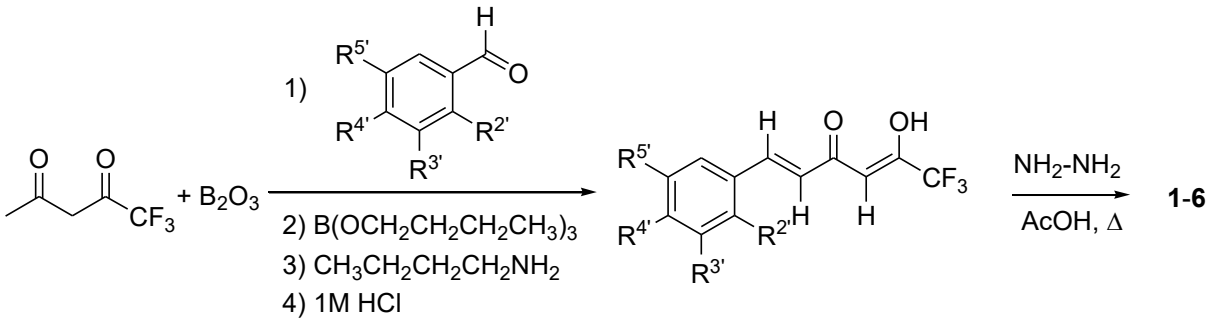

Fig. 3. The synthetic procedure.

Structure and NMR spectra

^{1}H NMR, ^{13}C NMR, ^{15}N NMR and ^{19}F NMR data, chemical shifts and coupling constants, of the studied pyrazoles are gathered in Tables 1-4. The attribution of the chemical shifts was based on the multiplicity of the signals as well as on the cross-peaks observed in the 2D (^{1}H-^{13}C) gs-HMQC and 2D (^{1}H-^{13}C) gs-HMBC spectra.

The assignment of the pyrazole ring carbon atoms did not present special difficulty due to the existing coupling constant $^{2}J_{CF3} \approx 36.5$ Hz of those carbons bonded to the CF_3 fluorine nuclei, and the C-styryl /H7 cross-peaks observed in the 2D (^{1}H-^{13}C) gs-HMBC spectra (see the example shown in Fig. 4).

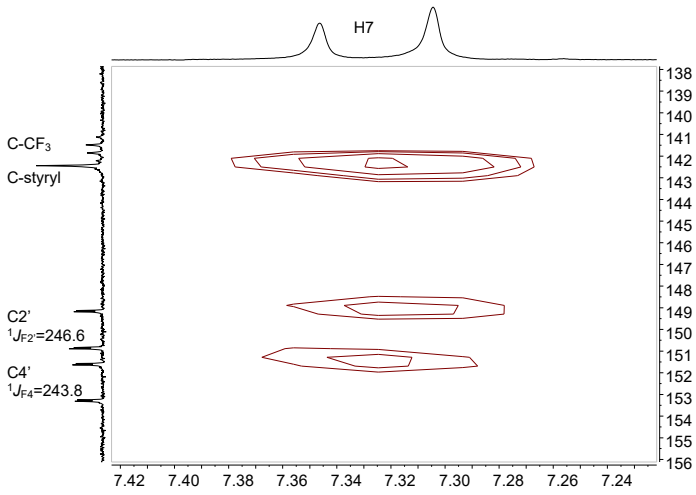

Fig. 4. 2D (^{1}H-^{13}C) gs-HMBC spectra recorded for compound **3**.

The signals corresponding to the CF_3 group appear at around 121 ppm, as quartets with a coupling constant of ~ 268 Hz. In what concerns the nuclei of the styryl group two important remarks must be pointed out: i) the chemical shift of C7 is influenced by the presence of fluorine in position 2, with values diminishing from ~130 (compounds **2**, **4**, **5**) to ~123 (compounds **1**, **3**, **4**) as reported in Table 2; ii) in compound **3**, it has been possible to discriminate between C2' (150.4, $^{1}J_{F2'}$ = 246.6) and C4' (152.1, $^{1}J_{F4'}$ = 243.8), on the basis of the cross peak observed between C2 'and H7 (7.32) (Fig. 4).

The coupling constants ^{n}J(HF) were determined both in the ^{1}H-NMR and in the ^{19}F-NMR spectra (Tables 1 and 4). Coupling constants through one bond, ^{1}J(CF), in pyrazoles **1**-**5** follow the order: $^{1}J_{C2F2}$ (247 Hz) > $^{1}J_{C4F4}$ (245 Hz) > $^{1}J_{C3F3}$ (240 Hz), similar to that observed in the mono and difluorinated starting aldehydes [49]. Regarding the coupling constants via two bonds, ^{2}J(CF), they vary from 10.0 Hz in compound **3** to 26.8 Hz in compound **4**; the magnitude of *J* diminishes when going from a **C**H-C**F** to a **C**R-C**F**. The ^{3}J(CF) coupling constants depend also on the substitution

pattern, with values between 12.1 Hz for **1** and **4** (**C**-CH-C**F**), and 1.6 Hz for **5** (**C**-C(OMe)-C**F**) (Tables 2 and 3).

Table 1
^{1}H NMR in solution of pyrazoles **1**-**6** (chemical shifts δ in ppm, J coupling constants in Hz) at 300 K.

	1	**2**	**3**	**4**	**5**	**6**	
Solvent	DMSO-d_6	DMSO-d_6	DMSO-d_6	DMSO-d_6	DMSO-d_6	DMSO-d_6	HMPA-d_{18}
NH	13.73	13.71	13.85	13.80	13.70	13.64	14.50
H4	6.89 (s)	6.83 (s)	6.96 (s)	6.88 (s)	6.88 (s)	6.81 (s)	6.85 (s)
H6	6.96 (d) $^{3}J_{H7}$=16.8	6.92 (d) $^{3}J_{H7}$=16.7	7.10 (d) $^{3}J_{H7}$=16.8	7.03 (d) $^{3}J_{H7}$=16.7	7.09 (d) $^{3}J_{H7}$=16.6	6.90 (d) $^{3}J_{H7}$=16.6	7.02 (d) $^{3}J_{H7'}$=16.6
H7	7.26 (d) $^{3}J_{H6}$=16.8	7.18 (d) $^{3}J_{H6}$=16.7	7.32 (d) $^{3}J_{H6}$=16.8	7.25 (dd) $^{3}J_{H6'}$=16.7 $^{5}J_{F5'}$=1.2	7.27 (d) $^{3}J_{H6}$=16.6	7.18 (d) $^{3}J_{H6}$=16.6	7.50 (d) $^{3}J_{H6'}$=16.6
H2'	---	7.36 (dd) $^{4}J_{H6'}$=2.0 $^{3}J_{F3'}$=12.5	---	---	7.34 (dd) $^{4}J_{H6'}$=2.2 $^{4}J_{F4'}$=8.4	7.12 (d) $^{4}J_{H6'}$=2.0	7.11 (d) $^{4}J_{H6'}$=1.8
H3'	6.61 (dd) $^{3}J_{F2'}$=12.9 $^{4}J_{H5'}$=2.4	---	---	6.79 (dd) $^{3}J_{F2'}$=11.8 $^{4}J_{F5'}$=7.4	3.89 (OMe)	3.82 (OMe)	3.80 (OMe)
4'-OH	10.20	10.14	---	10.68	---	9.27	10.42
3'-OH	---	---	10.29	---	---		
H5'	6.66 (dd) $^{3}J_{H6'}$=8.5 $^{4}J_{H3'}$=2.4	6.95 (dd) $^{3}J_{H6'}$=8.3 $^{4}J_{F3'}$=9.3	7.15-7.04 (m)	---	7.22 (dd) $^{3}J_{H6'}$=8.4 $^{3}J_{F4'}$=11.4	6.78 (d) $^{3}J_{H6'}$=8.1	6.88 (d) $^{3}J_{H6'}$=8.3
H6'	7.49 (dd) $^{4}J_{F2'}$=9.2 $^{3}J_{H5'}$=8.5	7.16 (dd) $^{3}J_{H5'}$=8.3 $^{4}J_{H2'}$=2.0	7.15-7.04 (m)	7.53 (dd) $^{3}J_{F5'}$=12.0 $^{4}J_{F2'}$=7.3	7.08 (ddd) $^{3}J_{H5'}$=8.4 $^{4}J_{H2'}$=2.2 $^{4}J_{F4'}$= 4.5	6.95 (dd) $^{3}J_{H5'}$=8.1 $^{4}J_{H2'}$=2.0	6.93 (dd) $^{3}J_{H5'}$=8.3 $^{4}J_{H2'}$=1.8

Table 2
^{13}C and ^{15}N NMR in solution and solid state of pyrazoles **1**-**3** (chemical shifts δ in ppm, J coupling constants in Hz) at 300 K.

	1		**2**		**3**	
Solvent	DMSO-d_6	CPMAS	DMSO-d_6	CPMAS	DMSO-d_6	CPMAS
C-CF_3	141.6 $^{2}J_{CF3}$=36.9	141.7	141.6 $^{2}J_{CF3}$=36.9	142.1	141.7 $^{2}J_{CF3}$=36.7	142.4
C4	101.1 ^{1}J=179.8	102.1 (+) 99.8 (–)	101.0 ^{1}J=180.4	99.0	101.8 ^{1}J=180.7	100.7 99.1
C-styryl	143.0	145.1 (–) 143.1 (+)	142.8	143.6	142.4	144.5 143.7
CF_3	121.7 $^{1}J_{F}$=268.3	122 [a]	121.7 $^{1}J_{F}$=268.0	120 [a]	123.0 $^{1}J_{F}$=268.1	121.5 [a]
C6	113.6 ^{1}J=157.1 $^{4}J_{F2'}$=5.6	113.8 (–) 111.9 (+)	112.7 ^{1}J=155.0	110.3	116.6 [a] ^{1}J=154.1 $^{4}J_{F2'}$=4.1	115.4

C7	124.3 ^{1}J=154.8 $^{3}J_{F2'}$=1.8	125.6 (+) 122.2 (–)	130.9 ^{1}J=151.1 $^{4}J_{F3'}$=1.8	133.4	123.6 ^{1}J=153.1	120.0
C1'	114.4 $^{2}J_{F2'}$=12.4	116.5 (+) 115.1 (–)	127.9 $^{3}J_{F3'}$=6.4	127.6	120.6 $^{2}J_{F2'}$=10.0 $^{4}J_{F4'}$=3.3	120.0
C2'	160.7 $^{1}J_{F2'}$=248.5	162.0 (–) 159.3 (+)	113.6 ^{1}J=159.6 ^{3}J~^{3}J~5.5 $^{2}J_{F3'}$=18.7	110.3	150.4 $^{1}J_{F2'}$=246.6 $^{3}J_{F4'}$=6.0	151.3 149.4
C3'	102.8 ^{1}J=161.8 ^{3}J=4.8 $^{2}J_{F2'}$=24.3	102.1 (+) 99.8 (–)	151.2 $^{1}J_{F3'}$=241.2	153.4 151.0	134.0 $^{2}J_{F2'}$=$^{2}J_{F4'}$=16.1	133.0
C4'	159.3 $^{3}J_{F2'}$=12.2	157.7 (+) 153.2 (-)	145.4 $^{2}J_{F3'}$=12.4	145.2	152.1 $^{1}J_{F4'}$=243.8 $^{3}J_{F2'}$=5.9	152.5 151.3
C5'	112.3 ^{1}J=161.8 ^{3}J=4.9 $^{4}J_{F2}$=2.6	111.9 (+) 110.2 (–)	118.0 ^{1}J=159.9 $^{3}J_{F3'}$=3.1	117.0	111.9 ^{1}J=165.7 $^{2}J_{F4'}$=19.1 $^{4}J_{F2'}$=3.1	111.5
C6'	128.6 ^{1}J=160.0 ^{3}J=5.6 $^{3}J_{F'2'}$=5.6	132.5 (–) 130.2 (+)	123.7 ^{1}J=160.0 $^{4}J_{3'}$=2.9	129.7	116.3 ^{1}J=166.2 $^{3}J_{F4}$=8.3 $^{3}J_{F2}$=3.5	111.5
NH	[b]	–171.8	[b]	–172.8	–171.8	–171.6
N	[b]	–103.0	[b]	–102.0	[b]	–100.3

[a] Broad signal.

[b] Not detected.

Table 3

^{13}C and ^{15}N NMR in solution and solid state of pyrazoles **4**-**6** (chemical shifts δ in ppm, J coupling constants in Hz) at 300 K.

	4		**5**		**6**		
Solvent	DMSO-d_6	CPMAS	DMSO-d_6	CPMAS	DMSO-d_6	HMPA-d_{18}	CPMAS
C-CF_3	141.7 $^{2}J_{CF3}$=37.3	142.3	141.7 $^{2}J_{CF3}$=36.2	142.6 141.4 140.6	141.6 $^{2}J_{CF3}$=36.6	141.9 $^{2}J_{CF3}$=36.5	143.1
C4	101.6	100.0	101.3 ^{1}J=181.0	99.6 99.1 98.7	100.6 ^{1}J=179.5	100.6	104.2
C-styryl	142.6	144.8	142.6	144.4	143.2	144.1	143.1
CF_3	121.7 $^{1}J_{F}$=268.1	122.6 [a]	121.7 $^{1}J_{F}$=268.1	121.5	121.8 $^{1}J_{F}$=268.1	122.8 $^{1}J_{F}$=267.6	120.3 [a]
C6	115.0	110.2	114.6 ^{1}J=160	113.9	111.3 ^{1}J=155.8	111.6	112.9
C7	123.0	122.6[a]	131.0 ^{1}J=155.4	131.7	132.2 ^{1}J=148.9	132.5	127.9
C1'	114.3 $^{2}J_{F2'}$=14.4	116.6 (–) 115.2 (+)	133.0 $^{4}J_{F4'}$=3.7	132.4	127.4	128.0	127.9

	$^3J_{F5'}$=6.7						
C2'	156.0 $^1J_{F2'}$=245.3 $^4J_{F5'}$=1.5	157.0 (+) 155.0 (–)	111.2 ^1J=159.9 $^3J_{H6'}$ ≈6.1 $^3J_{H7}$ ≈6.1 $^3J_{F4'}$=1.6	110.7 109.4 107.6	109.7 ^1J=156.0	111.6	108.9
C3'	105.0 $^2J_{F2'}$=26.8 $^3J_{F5'}$=3.3	104.9	147.4 $^2J_{F4'}$=11.0	147.9	147.4	148.8	146.3
R_3	---	---	56.0 ^1J=145.4	55.1 54.4 53.9	55.6 ^1J=144.3	56.1	55.2
C4'	146.3 $^2J_{F5'}$=14.7 $^3J_{F2'}$=12.1	146.0	151.1 $^1J_{F4'}$=246.5	153.1 150.6	147.9	149.7	146.3
C5'	148.0 $^1J_{F5'}$=238.0 $^4J_{F2'}$=2.1	150.3 (–) 147.8 (+)	116.2 ^1J=164.3 $^2J_{F4'}$=18.6	115.5 116.0	115.6 ^1J=159.4	116.0	114.4
C6'	113.6 $^2J_{F5'}$=21.3 $^3J_{F2'}$=5.6	110.2	119.8 ^1J=164.5 $^3J_{H2'}$≈6 $^3J_{H7}$≈6 $^3J_{F4'}$=6.8	121.5	120.6 ^1J=159.6	120.3	115.9
NH	–172.7	–173.0	[b]	–169.3 (2) –173.6 (1)	[b]	–170.2	–180.0
N	[b]	–98.3 (–) –103.5 (+)	[b]	–97.4 (1) –102.0 (2)	[b]	–80.2	–96.3

[a] Broad signal.

[b] Not detected.

Table 4

^{19}F NMR in solution and solid state of pyrazoles **1-6** (chemical shifts δ in ppm, J coupling constants in Hz).

Comp.	Solvent	CF_3	F2'	F3'	F4'	F5'
	DMSO-d_6	–61.0	–116.1 $^3J_{H3'}$=12.9 $^4J_{H6'}$=9.2			
1	MAS	–57.8 (1.5) –59.6 (1)	–106.9 (1); –111.3 (0.5) Mean: –108.0 (1.5) –114.4 (1)			
	DMSO-d_6	–60.5		–135.9 $^3J_{H2'}$=12.5 $^4J_{H5'}$=9.3		
2						
	MAS	–57.6		–136.1		
3	DMSO-d_6	–60.5	–135.8 $^4J_{FF}$=13.3 $^4J_{H6'}$=7.5[a]		–131.3 $^4J_{FF}$=13.3 $^4J_{H5'}$=10.1[a] $^5J_{H6'}$=6.0[a]	
	MAS	–59.1 –60.1 –61.0	–135.0 –137.4 –139.6		–128.9 –130.9 –132.4	

4	DMSO-*d*$_6$	–60.5	–120.8 $^5J_{FF}$=15.1 $^3J_{H3'}$=11.8 $^4J_{H6'}$=7.3		–140.5 $^5J_{FF}$=15.1 $^3J_{H6'}$=12.0 $^4J_{H3'}$=7.4 $^5J_{H7}$=1.2
	MAS	–57.7 (1) –59.8 (2)	–110.7 (–) –113.4 (–) –117.4 (+) –120.8 (+)		–135.9 (+) –138.7 (+) –141.7 (–) –143.7 (–)
5	DMSO-*d*$_6$	–60.5		–134.7 $^3J_{H5'}$=11.4 $^4J_{H2'}$=8.4 $^4J_{H6'}$=4.5	
	MAS	–57.3 (2) –59.4 (1)		–131.4 –133.3 –134.7	
6	DMSO-*d*$_6$	–60.5			
	HMPA-*d*$_{18}$	–61.6			
	MAS	–61.5			

[a] Measured only in ^{19}F NMR.

Finally, to illustrate the spectra we have included two figures, one for ^{15}N CPMAS (Fig. 5) and the other for ^{19}F MAS (Fig. 6).

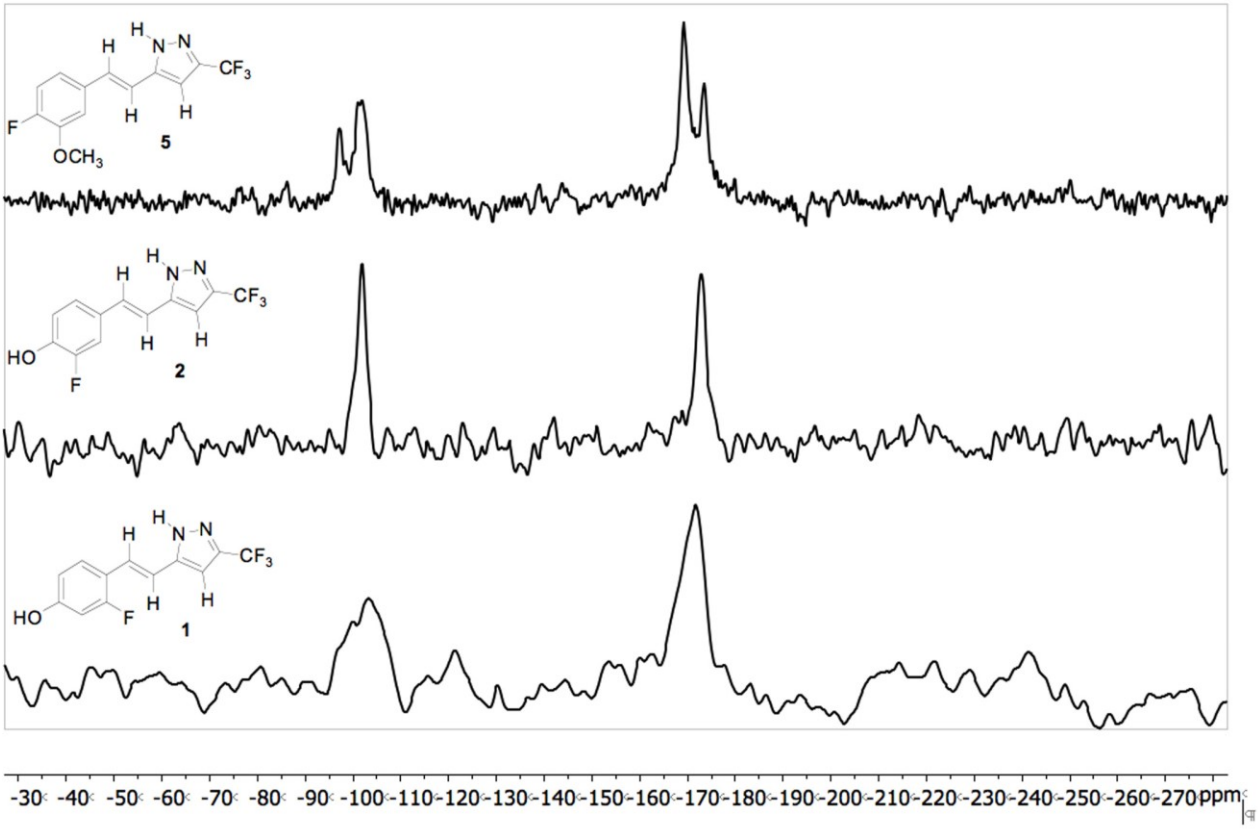

Fig. 5. ^{15}N CPMAS NMR spectra of compounds **1**, **2** and **5**.

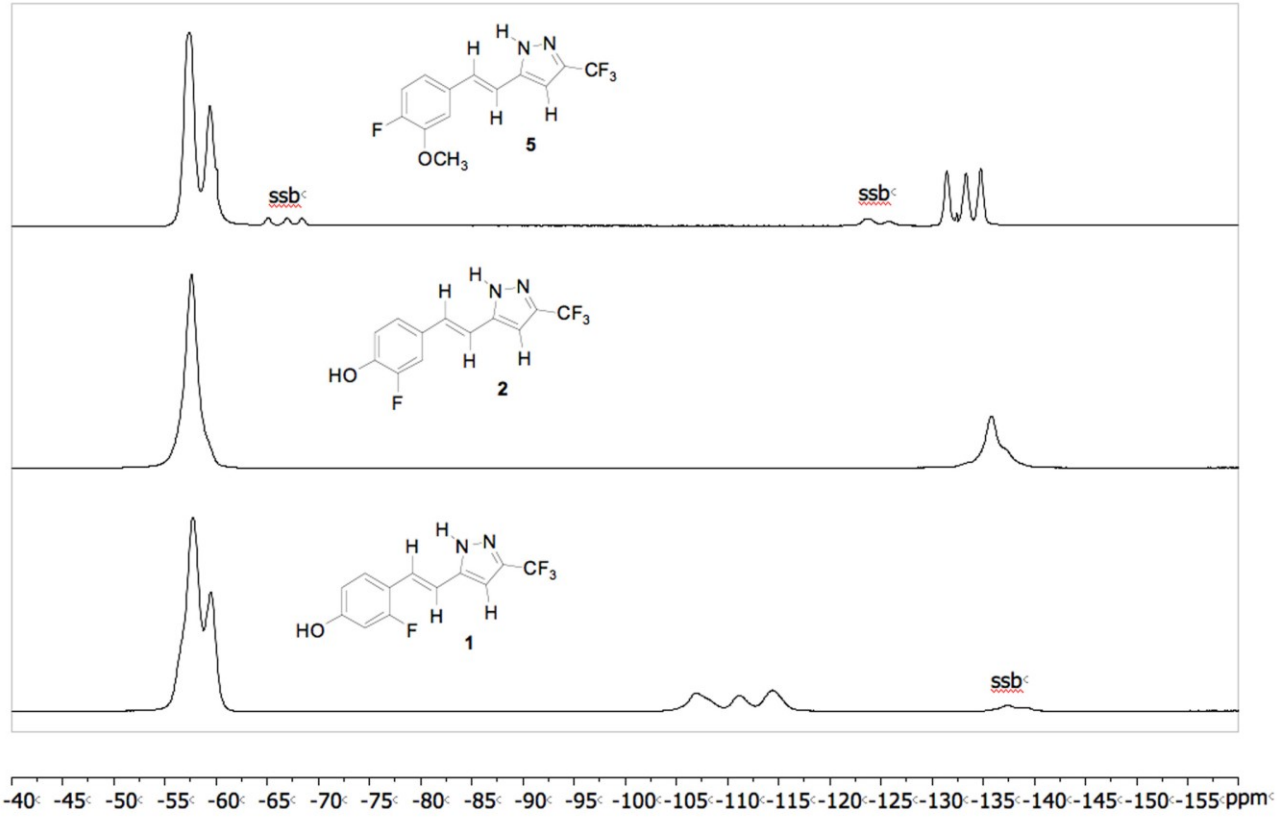

Fig. 6. ^{19}F MAS NMR spectra of compounds **1**, **2** and **5**.

*Tautomerism of pyrazoles **1-6***

The tautomerism represented in Fig. 2 is a simplification because besides the annular tautomerism (**a**/**b**), there exist conformational rotations about the C5-C6 and C7-C1' single bonds (Fig. 7). The relative energies associated with those geometries are reported in Table 5 (the corresponding absolute energies in hartrees are in the Supplementary Material, Table T1). We have transformed Table 5 into a Free-Wilson, or absence-presence matrix (Supplementary Material, Table T2) and analyzed it.

The 48 E_{rel} lead to the following equation (missing variables correspond to non-significant ones):

E_{rel} (kJ·mol^{-1}) = –(5.1±0.4) tautomer **a** + (2.8±0.6) 2'F + (1.5±0.5) 3'F + (4.6±0.5) 3'OMe + (3.0±0.6) 4'OH, R^2 = 0.91 (1).

This means that tautomer **a** is, on average, 5.1 kJ·mol^{-1} more stable than tautomer **b**. All substituents on the phenyl ring favor tautomer **a**, i.e. increase the difference in **b**–**a** E_{rel}. Another way is to analyze only the six **a**/**b** pairs where the difference in E_{rel} is minimal (red/blue pairs):

E_{rel} (kJ·mol^{-1}) = (0.8±0.6) 2'F + (0.8±0.7) 3'OMe + (1.4±0.7) 4'OH – (1.2±0.6) 5'F + (2.7±0.9) conformation 7-1' (from *sZ* to *sE*), R^2 = 0.998 (2).

Comparing eqs. (1) and (2), it appears that reducing 48 to 6 **a**/**b** pairs, most coefficients become smaller (from 2.8 to 0.8, from 1.5 to non-significant, from 4.6 to 0.8 kJ·mol^{-1}) although one of them, 5'F changes from non-significant to –1.2 kJ·mol^{-1}. A perusal of Fig. 7 and Table 5 shows that the most stable **a** tautomers have *sZ*-7-1' conformation while the most stable **b** tautomers have *sE*-7-1' conformation.

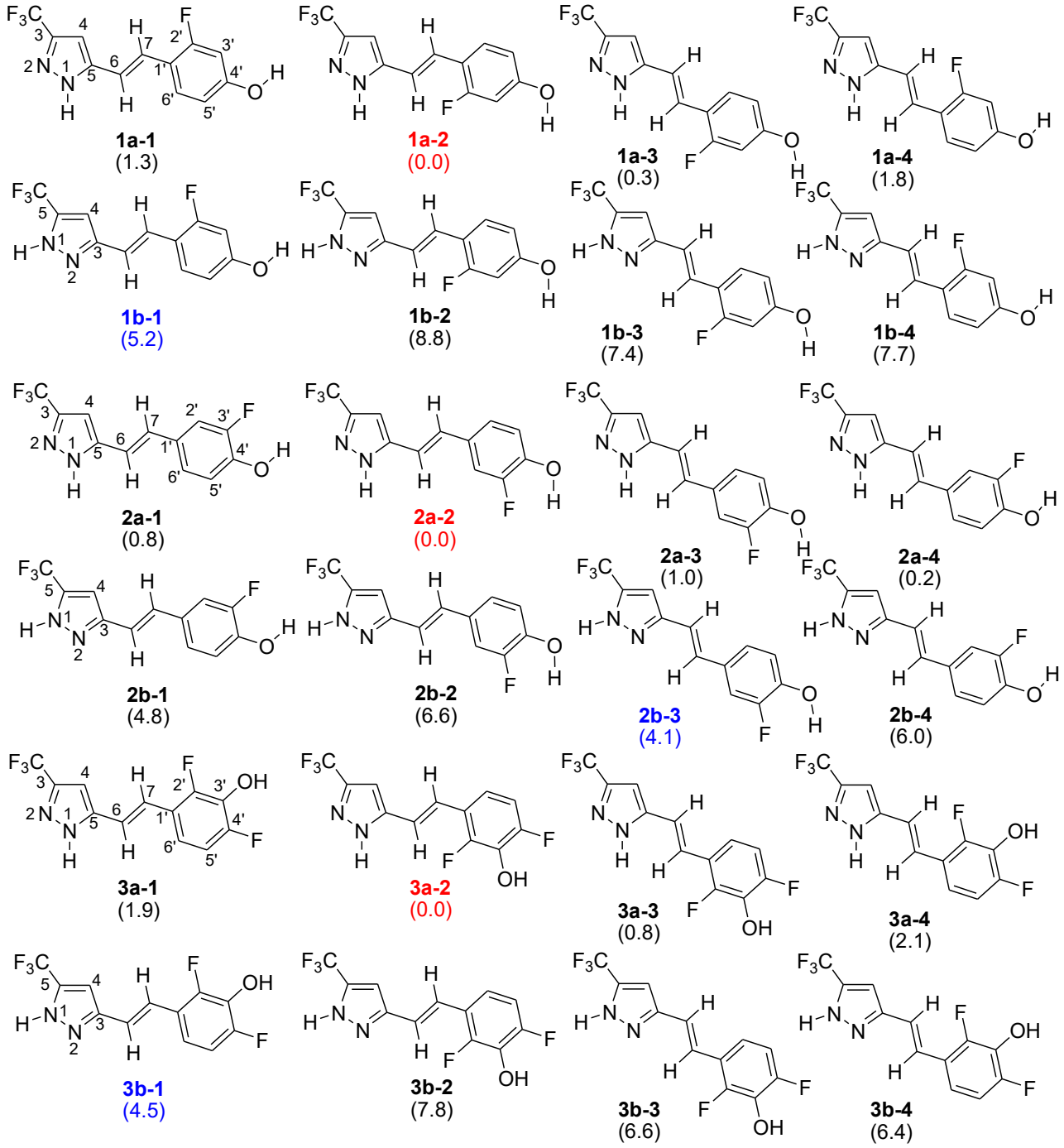
1a-1 (1.3)
1a-2 (0.0)
1a-3 (0.3)
1a-4 (1.8)
1b-1 (5.2)
1b-2 (8.8)
1b-3 (7.4)
1b-4 (7.7)
2a-1 (0.8)
2a-2 (0.0)
2a-3 (1.0)
2a-4 (0.2)
2b-1 (4.8)
2b-2 (6.6)
2b-3 (4.1)
2b-4 (6.0)
3a-1 (1.9)
3a-2 (0.0)
3a-3 (0.8)
3a-4 (2.1)
3b-1 (4.5)
3b-2 (7.8)
3b-3 (6.6)
3b-4 (6.4)

Fig. 7. Cont.

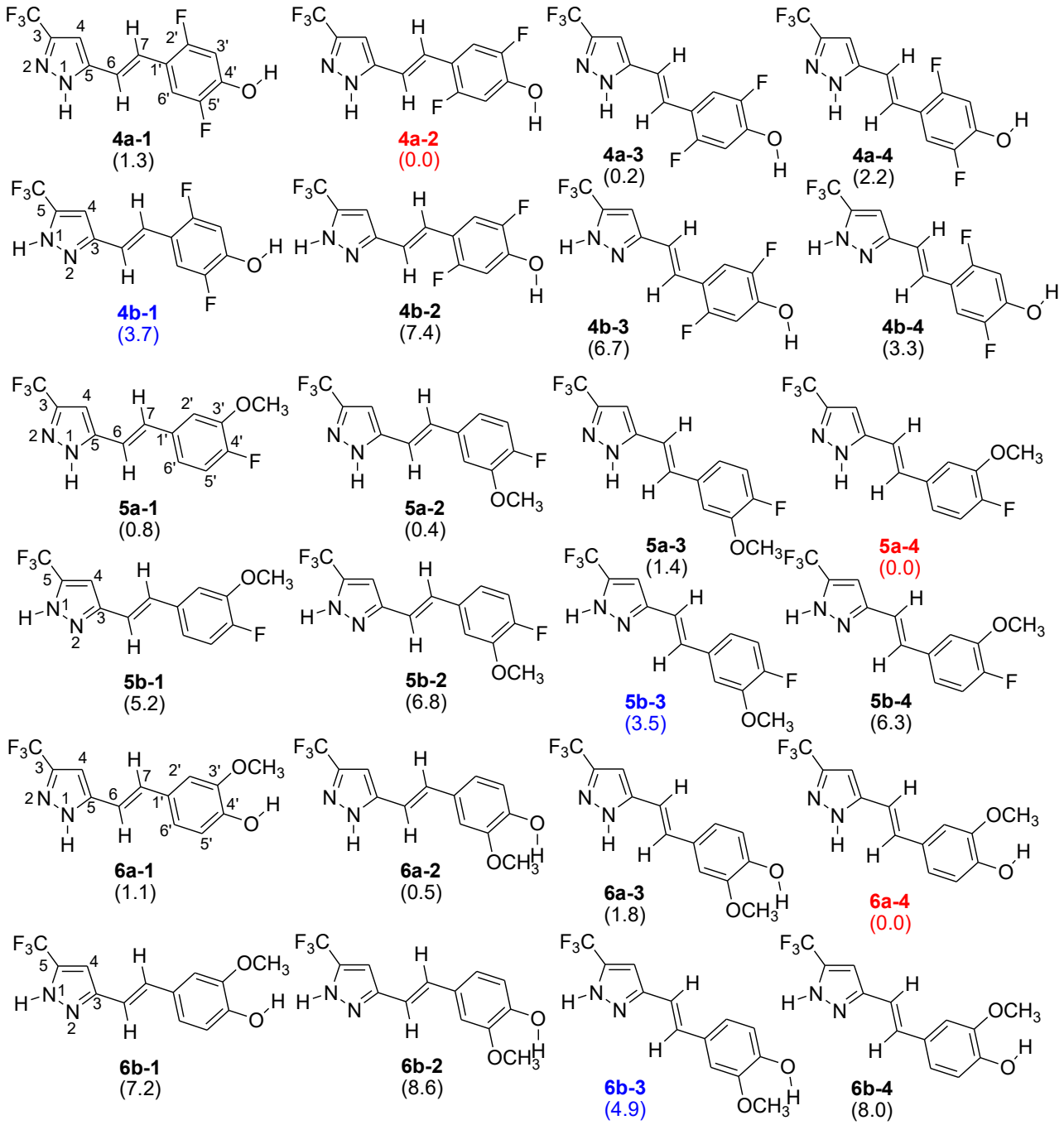

Fig. 7. Different tautomers (series **a** and **b)** and conformers of pyrazoles **1-6.**

Table 5

Relative stabilities (kJ·mol^{-1}) of the different tautomers and conformers. In red the most stable ones (always **a**); in blue the most stable **b** tautomer.

Comp.	Taut	2'-F	3'-F	4'	5'	5-6	7-1'	E_{rel}
1a-1	3-CF_3	F	H	OH	H	*sE*	*sE*	1.3
1a-2	3-CF_3	F	H	OH	H	*sE*	*sZ*	**0.0**
1a-3	3-CF_3	F	H	OH	H	*sZ*	*sE*	0.3
1a-4	3-CF_3	F	H	OH	H	*sZ*	*sZ*	1.8
1b-1	5-CF_3	F	H	OH	H	*sE*	*sE*	5.2
1b-2	5-CF_3	F	H	OH	H	*sE*	*sZ*	8.8
1b-3	5-CF_3	F	H	OH	H	*sZ*	*sE*	7.4
1b-4	5-CF_3	F	H	OH	H	*sZ*	*sZ*	7.7

2a-1	3-CF_3	H	F	OH	H	*sE*	*sE*	0.8
2a-2	3-CF_3	H	F	OH	H	*sE*	*sZ*	**0.0**
2a-3	3-CF_3	H	F	OH	H	*sZ*	*sE*	1.0
2a-4	3-CF_3	H	F	OH	H	*sZ*	*sZ*	0.2
2b-1	5-CF_3	H	F	OH	H	*sE*	*sE*	4.8
2b-2	5-CF_3	H	F	OH	H	*sE*	*sZ*	6.6
2b-3	5-CF_3	H	F	OH	H	*sZ*	*sE*	4.1
2b-4	5-CF_3	H	F	OH	H	*sZ*	*sZ*	6.0
3a-1	3-CF_3	F	F	OH	H	*sE*	*sE*	1.9
3a-2	3-CF_3	F	F	OH	H	*sE*	*sZ*	**0.0**
3a-3	3-CF_3	F	F	OH	H	*sZ*	*sE*	0.8
3a-4	3-CF_3	F	F	OH	H	*sZ*	*sZ*	2.1
3b-1	5-CF_3	F	F	OH	H	*sE*	*sE*	4.5
3b-2	5-CF_3	F	F	OH	H	*sE*	*sZ*	7.8
3b-3	5-CF_3	F	F	OH	H	*sZ*	*sE*	6.5
3b-4	5-CF_3	F	F	OH	H	*sZ*	*sZ*	6.4
4a-1	3-CF_3	F	H	OH	F	*sE*	*sE*	1.3
4a-2	3-CF_3	F	H	OH	F	*sE*	*sZ*	**0.0**
4a-3	3-CF_3	F	H	OH	F	*sZ*	*sE*	0.2
4a-4	3-CF_3	F	H	OH	F	*sZ*	*sZ*	2.2
4b-1	5-CF_3	F	H	OH	F	*sE*	*sE*	3.7
4b-2	5-CF_3	F	H	OH	F	*sE*	*sZ*	7.4
4b-3	5-CF_3	F	H	OH	F	*sZ*	*sE*	6.7
4b-4	5-CF_3	F	H	OH	F	*sZ*	*sZ*	6.3
5a-1	3-CF_3	H	OCH_3	F	H	*sE*	*sE*	0.8
5a-2	3-CF_3	H	OCH_3	F	H	*sE*	*sZ*	0.4
5a-3	3-CF_3	H	OCH_3	F	H	*sZ*	*sE*	1.4
5a-4	3-CF_3	H	OCH_3	F	H	*sZ*	*sZ*	**0.0**
5b-1	5-CF_3	H	OCH_3	F	H	*sE*	*sE*	5.2
5b-2	5-CF_3	H	OCH_3	F	H	*sE*	*sZ*	6.8
5b-3	5-CF_3	H	OCH_3	F	H	*sZ*	*sE*	3.5
5b-4	5-CF_3	H	OCH_3	F	H	*sZ*	*sZ*	6.3
6a-1	3-CF_3	H	OCH_3	OH	H	*sE*	*sE*	1.1
6a-2	3-CF_3	H	OCH_3	OH	H	*sE*	*sZ*	0.5
6a-3	3-CF_3	H	OCH_3	OH	H	*sZ*	*sE*	1.8
6a-4	3-CF_3	H	OCH_3	OH	H	*sZ*	*sZ*	**0.0**
6b-1	5-CF_3	H	OCH_3	OH	H	*sE*	*sE*	7.2
6b-2	5-CF_3	H	OCH_3	OH	H	*sE*	*sZ*	8.6
6b-3	5-CF_3	H	OCH_3	OH	H	*sZ*	*sE*	4.9
6b-4	5-CF_3	H	OCH_3	OH	H	*sZ*	*sZ*	8.0

*Relationships between experimental and calculated chemical shifts of pyrazoles **1-6***

We have compared the ^{1}H, ^{13}C, ^{15}N (when available) and ^{19}F chemical shifts with those calculated for the structures of Fig. 7 (see Table T3 of the Supplementary Material). We have selected the two major isomers, the red and the blue.

In the case of compound **3**, the conformer with the 3'-OH pointing towards F2' fits slightly better than that with 3'-OH pointing towards F4'. The results of the regression are reported in Table 6, where two dummy columns have been added for the NH and OH protons that otherwise cannot be compared with our calculations as well as a third dummy for the ^{15}N chemical shift of the pyrazole NH involved in hydrogen bonds (in DMSO-*d*$_6$ solution, no N ^{15}N NMR signal was observed). The results of the multiple regression analyses are reported in Table 6.

Table 6
Results of the multiple regressions (n = 22 or 23, R^2 = 0.999); the last column reports the calculated differences in energy of Table 5 (blue values).

Comp.	**a-2**	**a-4**	**b-1**	**b-3**	ΔG kJ·mol^{-1}	NH	OH	^{15}N (NH)	**b–a** kJ·mol^{-1}
1	0.7±0.1		0.3±0.1		2.1	4.9±2.7	6.3±2.7	---	5.2
2	0.9±0.1			0.1±0.1	5.5	5.0±3.4	5.4±3.4	---	4.1
3	0.6±0.2		0.4±0.2		1.0	5.0±3.8	5.8±3.8	13.0±4.3	4.5
4	0.55±0.15		0.45±0.15		0.5	5.0±3.5	6.0±3.5	12.8±4.0	3.7
5		0.6±0.1		0.4±0.1	1.0	4.5±2.9	---		3.5
6		0.7±0.1		0.3±0.1	2.1	4.4±2.7	3.8±2.7		4.9

Note that the sum of the coefficients, excluding the dummies, is equal to 1. At 300 K, the differences in energy determined by NMR are lower than those directly calculated (Table 5) but still in the same range. Besides, if one excludes compound **2**, they are roughly proportional [**b–a** = (2.8±0.5)*ΔG, n = 5, R^2 = 0.90]. This is rather satisfying taking into account that ΔG values correspond to experiments carried out in DMSO while **b–a** differences correspond to gas phase calculations.

Concerning the solid state (see Table T4 of the Supplementary Material) two cases should be differentiated: i) compounds with no split signals; ii) compounds where most signals are split. Since the data correspond to ^{13}C, ^{15}N and ^{19}F, it is not necessary to add dummy columns corresponding to the NH and OH protons, only for both ^{15}N CPMAS NMR signals.

The first case corresponds to pyrazoles **2** and **6** (Table 7). In the case of **2** the structure present in the solid state is **2-a2**, the same than in solution. In the case of **6**, the solid state contains **6-a3** and the solution **6-a4** (Table 6) that corresponds to a rotation about the 7-1' bond and that lies only 1.8 kJ·mol^{-1} higher in energy.

The second case corresponds to the remaining pyrazoles. In pyrazole **1** there is a clear difference in intensity close to 60-40, that allows to separate the signals in two groups, the (+) and the (–). The (+) corresponds to **1-a2** and the (–) to **1-a1**, i.e. to a rotation about the 7-1' bond and that lies only 1.3 kJ·mol^{-1} higher in energy. The case of pyrazole **4** is almost identical. Pyrazole **5** shows several signals that appear like triplets of the same intensity (for instance, the ^{13}C of the methoxy group, that of the C-CF_3, that of C4; the ^{19}F of F4') and in other cases as doublets of intensity 1:2, i.e., a 1:1:1 triplet with two signals superposed (for instance, the ^{13}C of C2', C4', the ^{15}N of both nitrogen atoms and the ^{19}F of the CF_3). We have found the best solution assuming the forms, **5-a1**, **5-a2** and **5-a4** (that present in solution) and reported the results in Table 7. The first two ones correspond to a 7-1' rotation and the third one to a 56 rotation.

The most complex case corresponds to pyrazole **3** because besides the conformations resulting from rotations about 5-6 and 7-1' there are the two conformations of the OH group (towards F2' and towards F4'). It results in 16 calculated values probably corresponding to three independent molecules in the unit cell (see Table T5 of the Supplementary Material) a problem too complex to be solved. Tentatively, we have adjusted all the data to a model involving two conformations of the O–H···F2' class and reported it in Table 7.

Table 7
Relationship between CPMAS and MAS NMR chemical shifts and calculated values for all structures of Fig. 7.

Comp.	Structure	N*H*	N	n	R^2
1, major (60%)	0.984±0.006 **a-2**	10.6±2.9	–27.0±2.7	16	1.000
1, minor (40%)	0.992±0.008 **a-1**	13.2±3.9	–26.1±3.7	16	0.999
2	0.985±0.008 **a-2**	10.8±4.2	–26.3±4.0	17	0.999

3	(0.38±0.20) **a-1** + (0.60±0.20) **a-2**	10.2±4.6	–26.7±4.6	27	0.999
4, major (66%)	0.972±0.100 **a-1**	8.0±5.7	–29.5±5.4	19	0.999
4, minor (33%)	0.973±0.008 **a-2**	7.1±4.5	–24.7±4.3	19	0.999
5 (33%)	0.994±0.008 **a-1**	13.8±3.0	–23.1±2.7	19	0.999
5 (33%)	0.998±0.008 **a-2**	14.6±2.9	–22.6±2.6	19	0.999
5 (33%)	0.997±0.008 **a-4**	24.5±3.2	–26.6±2.8	19	0.999

Some comments about the results reported in Table 7: i) some additional splittings remain, for instance, ^{19}F MAS of F2' in compound **1**; ii) we needed to use **b** tautomers; iii) if the N coefficient is relatively constant, that of the NH shows large variations (between 7.1 to 24.5 ppm), we have assigned these variations to the different kinds of N–H···N hydrogen bonds present in 1*H*-pyrazoles [50,51].

NOS inhibitory activity

NOS activity was measured following the conversion of L-^{3}H-arginine to L-^{3}H-citrulline according to the Bredt *et al*. [38] protocol and full details are given in the Experimental Section. The NOS inhibitory activities of the six pyrazoles (**1**-**6**) are gathered in Table 8 and represented in Fig. 8.

Table 8
Percentage of NOS inhibition using 50 µM/DMSO of pyrazoles.

Comp.	2'	3'	4'	5'	% nNOS	% iNOS	% eNOS
1	F	H	OH	H	29.1 ± 0.6	62.9 ± 10.3	56.8 ± 4.8
2	H	F	OH	H	47.4 ± 4.9	63.5 ± 7.1	52.6± 0.4
3	F	OH	F	H	52.9 ± 3.7	68.8 ± 3.0	40.2 ± 0.2
4	F	H	OH	F	34.6 ± 0.8	41.8 ± 3.5	47.9 ± 7.5
5	H	OCH_3	F	H	37.8 ± 0.7	52.8 ± 4.1	49.4 ± 3.4
6	H	OCH_3	OH	H	41.9 ± 1.6	53.3 ± 2.5	45.9 ± 0.3

All compounds, except **4**, present inhibition percentages of the iNOS isoform higher than 50%. Compound **3** shows the highest inhibitory activity with a value close to 70%, followed by those pyrazoles having only a fluorine atom, in positions 2' or 3' (**1**, **2**). With regard to the nNOS inhibitory activity, only two of the studied compounds show an inhibition of about 50% for this isoform (**2** and **3**).

Finally, concerning the eNOS, the compound presenting lower percentage of inhibition is **3** (40.2%) roaming in the other cases 50%. The monofluorinated pyrazoles **1** and **2** highlight among all compounds with inhibition percentages of 56.8 and 52.6%, respectively.

For the three isoforms, it results that the replacement of the 3'-methoxy group in **6** by a fluorine atom in **2** results in a slight increase in the percentage of inhibition.

In summary, the pyrazoles studied exhibit a major inhibition of the inducible iNOS isoform versus the constitutive isoforms nNOS and eNOS. Those with fluorine atoms at positions 2' or 3' show the highest inhibition percentages of this isoform, (*E*)-3(5)-[β-(2-fluoro-4-hydroxyphenyl)-ethenyl]-5(3)-trifluoromethyl-1*H*-pyrazole (**1**) being the most selective of eNOS and iNOS versus nNOS.

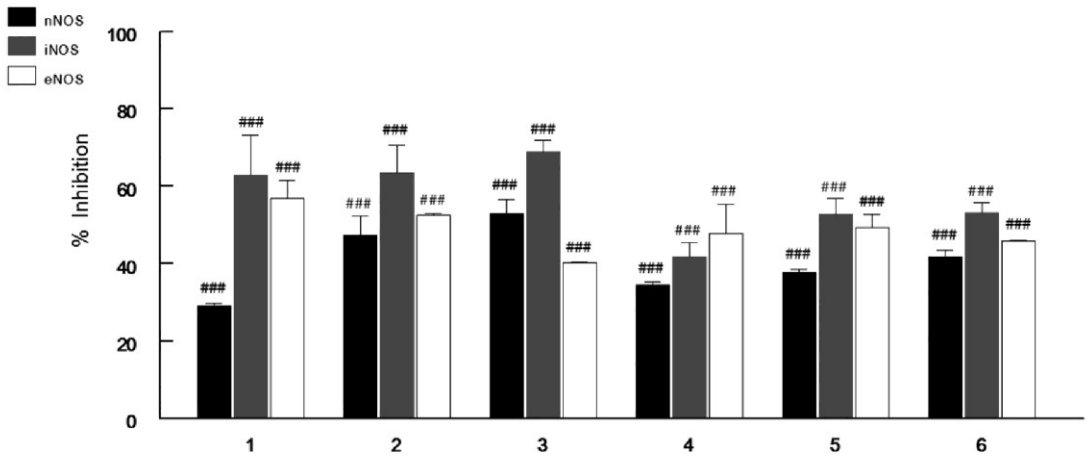

Fig. 8. Percentage of inhibition of nNOS, iNOS and eNOS activities in the presence of the tested curcuminoid pyrazoles (**1-6**) compared to control (0% inhibition). Experimental data represent the means ± S.E.M. of three independent experiments (n = 3), each one performed in triplicate $^{###}P < 0.001$ *vs.* control.

Conclusions

A new family of 1*H*-pyrazoles bearing at the tautomeric positions 3 and 5, trifluoromethyl and styryl substituents (with F, OH and OCH_3 substituents on the phenyl ring) have been prepared.

In DMSO solution, the tautomerism has been determined by a combination of ^{1}H, ^{13}C and ^{19}F NMR chemical shifts and GIAO/B3LYP/6-311++G(d,p) theoretical calculations. In most cases, the ^{15}N signals were not observed due to intermediates rates of tautomerism.

We have tried to carry out experiments of NMR crystallography [52] in order to determine the structure of these 1*H*-pyrazoles in the solid state without any support from X-ray crystallography. We feel that, even partially, we have been successfully.

In what concerns their NOS inhibitory activity, the most interesting compounds, in terms of potency and selectivity, are **1** (2'-F,4'-OH) (iNOS ≈ 63 %, nNOS ≈ 29%) and **3** (2',4'-diF,3'-OH) (iNOS ≈ 69 %, eNOS ≈ 40%).

There is no relationship between the different NOS activities (Table 7) and the tautomeric composition (Table 6).

Acknowledgments

This work has been financed by Ministerio de Economía y Competitividad of Spain (CTQ2014-56833-R, RD12/0043/0005, and PI13-00981) and Comunidad Autónoma de Madrid (Project MADRISOLAR2, ref. S2009/PPQ-1533). One of us (C. I. Nieto) is indebted to UNED for a predoctoral fellowship (FPI "Grupos de Investigación" UNED).

Appendix A. Supplementary material

Supplementary data associated with this article: Table T1 containing the absolute energies in $kJ \cdot mol^{-1}$ and hartrees of the different tautomers and conformers of Fig. 7 in the main text, Table T2 with the Free-Wilson matrix data, Table T3 with the calculated ^{1}H, ^{13}C, ^{15}N and ^{19}F NMR chemical shifts for the structures of Fig. 7 in the main text, Table T4 with the experimental ^{1}H, ^{13}C, ^{15}N and ^{19}F NMR chemical shifts in solid state of pyrazoles **1-6** versus the calculated values for the different tautomers and conformers, and T5 with the experimental ^{1}H, ^{13}C, ^{15}N and ^{19}F NMR chemical shifts in solid state of pyrazole **3** versus the calculated values for the different tautomers and conformers, can be found in the online version, at http://…

References

[1] B.B. Aggarwal, I.D. Bhatt, H. Ichikawa, K.S. Ahn, G. Sethi, K.S. Sandur, C. Sundaram,.N. Seeram, S. Shishodia, Curcumin - Biological and Medicinal Properties. Turmeric the genus curcuma. Vol. 45, Chapter 10, CRC Press, New York, 2007.

[2] P. Anand, S.G. Thomas, A.B. Kunnumakkara, C. Sundaram, K.B. Harikumar, B. Sung, S.T. Tharakan, K. Misra, I.K. Priyadarsini, K.N. Rajasekharan, B.B. Aggarwal, Biochem. Pharmacol. 76 (2008) 1590–1611.

[3] H. Itokawa, Q. Shi, A. Toshiyuki, S.L. Morris-Natschke, K.-H. Lee, Chin. Med. 3 (2008) 11. DOI:10.1186/1749-8546-3-11.

[4] T. Esatbeyoglu, P. Huebbe, I.M.A. Ernst, D. Chin, A.E. Wagner, G. Rimbach, Angew. Chem. Int. Ed. 51 (2012) 5308–5332.

[5] C. Subash, P. Sridevi, K. Wonil, B.A. Bharat, Clin. Exp. Pharmacol. Physiol. 39 (2012) 283–299.

[6] S.N.A. Bukhari, I.B. Jantan, M. Jasamai, W. Ahmad, M.W.B. Amjad, J. Med. Sci. 13 (2013) 501–513.

[7] S. Prasad, S.C. Gupta, A.K. Tyagi, B.B. Aggarwal, Biotechnol. Adv. 32 (2014) 1053–1064.

[8] K. Bairwa, J. Grover, M. Kania, S.M. Jachak, RSC Adv. 4 (2014) 13946–13978.

[9] M.K. Shanmugam, G. Rane, M.M. Kanchi, F. Arfuso, A. Chinnathambi, M.E. Zayed, S.A. Alharbi, B.K.H. Tan, A.P. Kumar, G. Sethi, Molecules 20 (2015) 2728–2769.

[10] L. Kong, K.I. Priyadarsini, H.-Y. Zhang, J Mol Struct (Theochem) 685 (2004) 111–116.

[11] P. Cornago, R.M. Claramunt, L. Bouissane, I. Alkorta, J. Elguero, Tetrahedron 64 (2008) 8089–8094.

[12] P. Galer, A. Golobic, J. Koller, B. Kosmrlj, B. Sket, Chem. Central J. 7 (2013) 107. DOI: 10.1186/1752-153X-7-107.

[13] E. Ferrari, M. Asti, R. Benassi, F. Pignedoli, M. Saladini, Dalton Trans. 42 (2013) 5304–5313.

[14] Y. Manolova, V. Deneva, L. Antonov, E. Drakalska, D. Momekova, N. Lambov, Spectrochim. Acta Part A 132 (2014) 815–820.

[15] P. Cornago, P. Cabildo, D. Sanz, R. M. Claramunt, M. C. Torralba, M. R. Torres, J. Elguero, Eur. J. Org. Chem. (2013) 6043–6054.

[16] V. Bertolasi, V. Ferrett, P. Gilli, X. Yao, C.-J. Li, New J. Chem. 32 (2008) 694–704.

[17] F. Blanco, I. Alkorta, K. Zborowski, J. Elguero, Struct. Chem. 18 (2007) 965–975.

[18] D.L. Flynn, T.R. Belliotti, A.M. Boctor, D.T. Connor, C.R. Kostlan, D.E. Nies, D.F. Ortwine, D.J. Schrier, J.C. Sircar, J. Med. Chem. 34 (1991) 518–525.

[19] M.C. Lozada, R.G. Enríquez, C.E. Lobato, B. Ortíz, M. Soriano-García, D. Gnecco, W.F. Reynolds, Heterocycles 65 (2005) 49–58.

[20] R. Narlawar, M. Pickhardt, S. Leuchtenberger, K. Baumann, S. Krause, T. Dyrks, S. Weggen, E. Mendelkow, B. Schmidt, B. ChemMedChem. 3 (2008) 165–172.

[21] Q. Chen, M. Prior, R. Dargush, A. Roberts, R. Riek, C. Eichmann, C. Chiruta, T. Akaishi, K. Abe, P. Maher, D. Schubert, Plos One 6 (2011) e27865. DOI: 10.1371/journal.pone.0027865.

[22] S.Y. Jadhav, R.B. Bhosale, S.P. Shirame, S.B. Patil, S.D. Kulkarni, Chem. Biol. Drug Des. 85 (2015) 377–384.

[23] R.M. Claramunt, L. Bouissane, M.P. Cabildo, M.P. Cornago, J. Elguero, A. Radziwon, C. Medina, Bioorg. Med. Chem. 17 (2009) 1290–1296.

[24] P. Cornago, P. Cabildo, R.M. Claramunt, L. Bouissane, E. Pinilla, M.R. Torres, J. Elguero, New J. Chem. 33 (2009) 125–135.

[25] Th. Eicher, S. Hauptmann, A. Speicher, The Chemistry of Heterocycles, 3rd edn.; Wiley-VCH:Weinheim, 2012.

[26] A. Weber, A. Casini, A. Heine, D. Kuhn, C.T. Supuran, A. Scozzafava, G. Klebe, J. Med. Chem. 47 (2004) 550–557.

[27] R. Betageri, Y. Zhang, R.M. Zindell, D. Kuzmich, T.M. Kirrane, J. Bentzien, M. Cardozo, A.J. Capolino, T.N. Fadra, T.N. Nelson, Z. Paw, D.-T. Shih, C.-K. Shih, L. Zuvela-Jalaska, G. Nabozny, D.S. Thomson, Bioorg. Med. Chem. Lett. 15 (2005) 4761–4769.
[28] N.V. Cozzi, S.D. Brandt, P.F. Deley, J.S. Partilla, R.B. Rothman, A. Tulzer, H.H. Sitte, M.H. Baumann, Eur. J. Pharmacol. 699 (2013) 180–187.
[29] J. Elguero, A. Fruchier, N. Jagerovic, A. Werner, Org. Prep. Proc. Int. 27 (1995) 33–74.
[30] A. Guzman-Perez, J.A. Pfefferkorn, E.C.Y. Lee, B.D. Stevens, G.E. Aspnes, J. Bian, M.T. Didiuk, K.J. Filipski, D. Moore, C. Perreault, M.F. Sammons, M. Tu, J. Brown, K. Atkinson, J. Litchfield, B. Tan, B. Samas, W.J. Zavadoski, C.T. Salatto, J. Treadway, Bioorg. Med. Chem. Lett. 23 (2013) 3051–3058.
[31] S. Fustero, A. Simón-Fuentes, O. Delgado, R. Román, Fluorinated Pyrazoles and Indazoles, Fluorine in Heterocyclic Chemistry, Vol. 1:5-Membered (V. Nenajdenko, ed.), Springer Int Publishing, Switzerland, 2014.
[32] P.L. McCormack, Drugs 71 (2011) 2457–2489.
[33] S. Berger, S. Braun, 200 and More NMR Experiments; Wiley-VCH: Weinheim, 2004.
[34] P.D. Murphy, J. Magn. Reson. 52 (1983) 343–345; ibid. 62 (1985) 303–308.
[35] L.B. Alemany, D.M. Grant, T.D. Alger, R.J. Pugmire, J. Am. Chem. Soc. 105 (1983) 6697–6704.
[36] E. Crespo, M. Macías, D. Pozo, G. Escames, M. Martin, F. Vives, J.M. Guerrero, D. Acuña-Castroviejo, FASEB J. 13(1999) 1537–1546.
[37] O.H. Lowry, N.J. Rosebrough, A.L. Farr, R.J. Randall, J. Biol. Chem. 193 (1951) 265–275.
[38] D.S. Bredt, S.H. Snyder, Proc. Natl. Acad. Sci. USA 86 (1989) 9030–9033.
[39] A.D. Becke, Phys. Rev. A 38 (1988) 3098–3100.
[40] A.D. Becke, J. Chem. Phys. 98 (1993) 5648–5652.
[41] C. Lee, W. Yang, R.G. Parr, Phys. Rev. B 37 (1988) 785–789.
[42] R. Ditchfield, W.J. Hehre, J.A. Pople, J. Chem. Phys. 54 (1971) 724–728.
[43] M.J. Frisch, J.A. Pople, J.S. Binkley, J. Chem. Phys. 80 (1984) 3265–3269.
[44] Gaussian 09, Revision **A.1**, M.J. Frisch, G.W. Trucks, H.B. Schlegel, G.E. Scuseria, M.A. Robb, J.R. Cheeseman, G. Scalmani, V. Barone, B. Mennucci, G.A. Petersson, H. Nakatsuji, M. Caricato, X. Li, H.P. Hratchian, A.F. Izmaylov, J. Bloino, G. Zheng, J.L. Sonnenberg, M. Hada, M. Ehara, K. Toyota, R. Fukuda, J. Hasegawa, M. Ishida, T. Nakajima, Y. Honda, O. Kitao, H. Nakai, T. Vreven, J.A. Montgomery, Jr., J.E. Peralta, F. Ogliaro, M. Bearpark, J.J. Heyd, E. Brothers, K.N. Kudin, V.N. Staroverov, R. Kobayashi, J. Normand, K. Raghavachari, A. Rendell, J.C. Burant, S.S. Iyengar, J. Tomasi, M. Cossi, N. Rega, N.J. Millam, M. Klene, J.E. Knox, J.B. Cross, V. Bakken, C. Adamo, J. Jaramillo, R. Gomperts, R.E. Stratmann, O. Yazyev, A.J. Austin, R. Cammi, C. Pomelli, J.W. Ochterski, R.L. Martin, K. Morokuma, V.G. Zakrzewski, G.A. Voth, P. Salvador, J.J. Dannenberg, S. Dapprich, A.D. Daniels, Ö. Farkas, J.B. Foresman, J.V. Ortiz, J. Cioslowski, D.J. Fox, Gaussian, Inc., Wallingford CT, 2009.
[45] A.M.S. Silva, R.M.S. Sousa, M.L. Jimeno, F. Blanco, I. Alkorta, J. Elguero, Magn. Reson. Chem. 46 (2008) 859–864.
[46] F. Blanco, I. Alkorta, J. Elguero, Magn. Reson. Chem. 45 (2007) 797–800.
[47] N. Fesno, R. Pérez, M.L. Jimeno, I. Alkorta, G. Sánchez-Sanz, J. Elguero, J.E. Del Bene, J. Heterocycl. Chem. 49 (2012) 1257–1259.
[48] R.M. Claramunt, P. Cornago, V. Torres, E. Pinilla, M.R. Torres, A. Samat, V. Lokshin, M. Valés, J. Elguero, J. Org. Chem. 71 (2006) 6881–6891.
[49] D. Sanz, C. Nieto, R.M. Claramunt, I. Alkorta, J. Elguero, Magn. Reson. Chem. (2015). DOI: 10.1002/mrc.4260.
[50] C. Foces-Foces, I. Alkorta, J. Elguero, Acta Crystallogr. Sect. B 56 (2000) 1018–1028.
[51] I. Alkorta, J. Elguero, C. Foces-Foces, L. Infantes, Arkivoc ii (2006) 15–30.
[52] R. K. Harris, R. E. Wasylishen, M. J. Duer, NMR Crystallography, John Wiley & Sons, Chichester, 2009.